Toxicology and Applied Pharmacology 404 (2020) 115203

Contents lists available at ScienceDirect

Toxicology and Applied Pharmacology

journal homepage: www.elsevier.com/locate/taap

Salinomycin promotes T-cell proliferation by inhibiting the expression and enzymatic activity of immunosuppressive indoleamine-2,3-dioxygenase in human breast cancer cells

Azubuike Peter Ebokaiwe[a,c,1], Emmanuel Mfotie Njoya[a,d,1], Yuwen Sheng[a], Zhonghui Zhang[e], Sheng Li[a], Zongyuan Zhou[a], Zhe Qiang[a], Ting Peng[a], Ahmed A. Hussein[f], Guolin Zhang[a], Xiaoxia Lu[a], Lin Li[b,*], Fei Wang[a,*]

[a] Center for Natural Products Research, Chengdu Institute of Biology, Chinese Academy of Sciences, Chengdu 610041, China
[b] Department of Laboratory Medicine, Sichuan Academy of Medical Sciences & Sichuan Provincial People's Hospital, Chengdu 610072, China
[c] Department of Chemistry/Biochemistry and Molecular Biology, Alex Ekwueme Federal University Ndufu Alike-, Ikwo, Nigeria
[d] Department of Biochemistry, Faculty of Science, University of Yaoundé I, P.O Box 812, Yaoundé, Cameroon
[e] College of Chemical Engineering, Sichuan University, Chengdu 610064, China
[f] Chemistry Department, Cape Peninsula University of Technology, Bellville Campus, Bellville 7537, Western Cape, South Africa

ARTICLE INFO

Keywords:
Indoleamine-2,3-Dioxygenase
Kynurenine
Salinomycin
Interferon γ
Breast cancer

ABSTRACT

Indoleamine 2,3 dioxygenase (IDO) is upregulated in many tumor types, including breast cancer, and plays a reputable role in promoting tumor immune tolerance. The importance of the immunosuppressive mechanism of IDO by suppressing T-cell function has garnered profound interest in the development of clinical IDO inhibitors. Herein, we established a screening method with cervical HeLa cells to induce IDO expression using interferon-γ (IFN-γ). After screening our chemical library, we found that salinomycin potently inhibited IFN-γ-stimulated kynurenine synthesis with IC_{50} values of 3.36–4.66 μM in both human cervical and breast cancer cells. Salinomycin lowered the IDO1 and IDO2 expression with no impact on the expression of tryptophan-2,3-dioxygenase. Interestingly, salinomycin potently repressed the IDO1 enzymatic activity by directly targeting the proteins in cells. Molecular docking revealed an alignment that favors nucleophilic attack of salinomycin in the catalytic domain of IDO1. Activation of the Janus kinase/signal transducer and activator of transcription (JAK/STAT) pathway by IFN-γ was significantly suppressed by salinomycin, via inhibiting the Jak1, Jak2, and STAT1/3 phosphorylation. Moreover, it inhibited IFN-γ-induced activation of the nuclear factor (NF)-κB pathway by inhibiting IκB degradation and NF-κB phosphorylation without affecting BIN1 expression. Furthermore, salinomycin significantly restored the proliferation of T cells co-cultured with IFN-γ-treated breast cancer cells and potentiated antitumor activity of cisplatin in vivo. These findings suggest that salinomycin suppresses kynurenine synthesis by inhibiting the catalytic activity of IDO1 and its expression by inhibiting the JAK/STAT and NF-κB pathways. Salinomycin warrants further investigation as a novel dual-functional IDO inhibitor for cancer immunotherapy.

1. Introduction

The implication of the metabolic conversion of tryptophan to kynurenine, which is vital in the control of intrinsic immunity and adaptive response, has recently gained attention. Many preclinical models have demonstrated that this immune tolerance pathway is regulated by enzymes, indoleamine-2,3-dioxygenase (IDO) and tryptophan-2,3-dioxygenase (TDO). Different signaling pathways have been implicated in the control of the expression of IDO, mainly the nuclear factor (NF)-κB pathway and the Janus-activated kinase-signal transducer and activator of transcription (JAK-STAT) pathway (Platten et al., 2015). Interferon (IFN)-γ, a product of T cells and natural killer cells activation found in the tumor microenvironment, has been described as a principal instigator of IDO1 expression in numerous cancer types in human, where tryptophan deprivation contributes to the antiproliferative effect of IFN-γ (Ozaki et al., 1988). The upregulation of

* Corresponding authors.
E-mail addresses: spphll@163.com (L. Li), wangfei@cib.ac.cn (F. Wang).
[1] These authors contributed equally to this work.

https://doi.org/10.1016/j.taap.2020.115203
Received 24 February 2020; Received in revised form 13 August 2020; Accepted 15 August 2020
Available online 19 August 2020
0041-008X/

IDO is observed in colorectal cancer, pancreatic cancer and non-small-cell lung cancer, and has a correlation with tumor progression, invasiveness, and poor clinical outcomes (Godin-Ethier et al., 2011). Because of the critical role of IDO in immune escape, the focus of immunomodulatory drugs in cancer is targeting the IDO pathway by suppressing the IDO enzyme activity/expression or halting its downstream signaling effects.

In recent years pharmaceutical firms and academic circles are intensifying efforts to develop novel IDO inhibitors. So far, discoveries of numerous IDO1 inhibitor scaffolds have been achieved through screening or structure-based strategy (Qian et al., 2016). Nevertheless, the challenges associated with developing pharmacological inhibitors of IDO are noteworthy, because none of IDO inhibitors can suppress both the enzymatic activity and expression of IDO at the same time. Epacadostat is one of the prominent inhibitors of IDO1 that is widely studied in clinical and preclinical trials (Komiya and Huang, 2018). Epacadostat and several other available IDO1 inhibitors that potently inhibit the enzymatic activity of IDO1 and are orally administered either alone or in combination have recently entered clinical trials (Hamid et al., 2017; Perez et al., 2017; Komiya and Huang, 2018). Despite the disappointing result of epacadostat in phase III clinical trials, Komiya and Huang (2018) suggested that the combination of epacadostat with other therapeutic agents with possible synergy and molecular classification of various response is essential to its future use in the field of immunotherapy; this is considering the possibility of the inhibitors of IDO1 to improve immunological response. The failure of epacadostat in phase III clinical trials has also been attributed to its specific selective inhibition of IDO1 catalytic activity and its lack of inhibitory effects on IDO2 and TDO (Ye et al., 2019; Günther et al., 2019). Thus, new drugs that can actively decrease both expression and enzymatic activity of IDO1 and its family of enzymes, IDO2 and TDO, should be developed.

The specific inhibitory effects of salinomycin against human breast cancer stem cells have been studied (Gupta et al., 2009). Further, it has been confirmed to restrain the survival of numerous types of cancer stem cells and cancer cells (Naujokat and Steinhart, 2012; Zhou et al., 2013; Dewangan et al., 2017). Although the underlying mechanisms of the anticancer effects of salinomycin is yet to be completely elucidated, several mechanisms have been linked to its anticancer effects. Salinomycin has been shown to inhibit the Wnt signaling pathway by suppressing LRP6 phosphorylation or β-catenin and p-GSK-3 expression (Lu et al., 2011; He et al., 2013). Salinomycin elicits induction of reactive oxygen species and membrane depolarization of the mitochondria, which in turn results in the stimulation of caspase-3, initiation of PARP-1 cleavage, and ultimately increased apoptosis (Kim et al., 2011a; Kim et al., 2011b). Salinomycin was also shown to increase cell death via autophagy, impede the NF-κB pathway, and trigger the p38 MAPK pathway (Zhou et al., 2013). Notably, salinomycin reduced the growth and progression of breast cancer cells via the NF-κB deregulation (Tyagia and Patro, 2019). Thus, it would be meaningful to determine whether this compound modulates IDO-mediated immune response in breast cancer. IDO expression is recurrent among high-grade, triple-negative breast cancers, thereby strongly implicating its involvement in breast cancer progression (Dill et al., 2018).

The need to identify novel inhibitors of IDO prompted the current study to perform cell-based screening with IFN-γ stimulation. The screening revealed that salinomycin is a potential effective inhibitor of IFN-γ-stimulated kynurenine synthesis. Further, we determined the potential inhibitory effects of salinomycin on IDO1/IDO2 and TDO2 activity/expression in human breast cancer cells and the regulatory pathways. The findings herein will contribute to existing knowledge regarding the underlying molecular and biochemical mechanisms involved in the anticancer effects of salinomycin and provide new therapeutic means for cancer immunotherapy.

2. Materials and methods

2.1. Reagents

Human IFN-γ (#Z02915–50) or mouse IFN-γ (#Z02916–20) was obtained from GenScript (Piscataway, NJ, USA). JAK inhibitor I (#420099) was purchased from Calbiochem (Bilerica, MA, USA). Epacadostat (#S7910) and Bay 11–7082 (#S2913) were purchased from Selleck Chemicals (Shanghai, China). pCMV3-IDO1 (#HG13612-CF), IDO2 (#HG13614-CF) or TDO2 (HG13215-CF) plasmids were obtained from Sino Biological (Beijing, China). The control vector, pSV-β-galactosidase was obtained from Promega (Madison, WI, USA). Anti-IDO1 (#13268-I-AP), Anti-IDO2 (#25053–1-AP), Anti-TDO2 (#15880-I-AP), anti-BIN1 (#15880-I-AP), anti-SOCS3 (#14025–1-AP), anti-IκBα/β (#12660–1-AP), and anti-GAPDH (#10494–1-AP) antibodies were purchased from Proteintech (Wuhan, China). Anti-STAT3 (phospho-Tyr705, #11045), anti-JAK1 (phospho-Tyr 1022, #11149), anti-JAK2 (phospho-Y1007/1008, #13352), anti-NFκB-p65 (#48498), anti-SOCS1 (#24399) and anti-CD8 (#47992) antibodies were purchased from Signalway Antibody (Baltimore Ave, USA). Anti-STAT3 (#ET1607–38) antibody was purchased from HuaAn Biotechnology (Hangzhou, China), anti-JAK1 (#3344), anti-JAK2 (#3230), and anti-IκBα (phospho-Ser32/36, #9246), anti-NFκB-p65 (phospho-Ser 536, #3033) antibodies were purchased from Cell Signaling Technology (Beverly, MA, USA).

2.2. Cell culture and transfection

HeLa cells, MDA-MB 231 and MCF-7 cells, and HEK293A cells were purchased from Cell Bank of Chinese Academy of Science (Shanghai, China). 4 T1 cells were purchased from Procell Life Science & Technology Co., Ltd. (Wuhan, China). The cells were maintained in Dulbecco's modified Eagle's medium (Hyclone, UT, USA) supplemented with 10% fetal bovine serum at 37 °C in a humidified atmosphere of 5% CO_2. The plasmid for pCMV-IDO1, IDO2 or TDO2 (0.5 μg) was transiently transfected by seeding HEK293A cells in 24-well plates co-transfected with 0.3 μg pSV-β-galactosidase plasmid respectively using lipofectamine 2000 transfection reagent according to the manufacturer's protocol (Invitrogen, Carlsbad, CA, USA). The differences in transfection effectiveness were derived by normalizing IDO activity to β-galactosidase activity.

2.3. IDO cellular assay

The cellular IDO assay was conducted following earlier protocol (Lin et al., 2016). Cancer cells seeded in a 96-well plate were allowed to attach for 24 h. Afterward, 2 h treatment of cells with compounds was followed by 24 h stimulation by IFN-γ (50 ng/mL). Dimethylsulfoxide (DMSO, 0.5%) and 25 nM epacadostat served as the negative and positive controls. After incubation for 24 h, 140 μL of the supernatant was mixed with 10 μL of 6.1 N trichloroacetic acid (TCA), and the mixture was incubated for 30 min at 50 °C. The reaction mixture was then centrifuged for 10 min at 2500 rpm to remove sediments. One hundred microliters of the supernatant was mixed with 100 μL of 2% (*w/v*) *p*-dimethylaminobenzaldehyde in acetic acid and measured at OD 480 nm using VarioskanFlash Multimode Reader (Thermo Fisher). The extrapolation of kynurenine concentration was carried out from the standard curve of L-kynurenine. The IC_{50} values were determined by nonlinear regression analysis with Prism 5 software (GraphPad Software Inc., San Diego, CA, USA).

2.4. Screening of chemical compound library

An in-house library of natural products or synthetic analogues with 1431 compounds (Tai et al., 2012) were screened for their inhibitory effect on kynureine synthesis by using cellular IDO assay in cell

supernatants. HeLa cells (1×10^5 cells/well) were seeded in 96-well plates and pretreated with 10 μg/mL of the various compounds from the library for 2 h before 1×10^3 U/mL IFN-γ stimulation for 24 h. Thereafter, cell supernatants were collected to measure the concentration of L-kynurenine. The inhibitory rate was extrapolated from a standard curve of kynurenine synthesis against absorbance.

2.5. TDO cellular assay

The cellular TDO assay was conducted following earlier protocol (Yang et al., 2019b). Cells were treated with certain concentrations of compounds and L-Trp (20 μg/mL) for 24 h. Then, cell culture medium (300 μL/well) was transferred to a tube and mixed with 90 μL TCA (30%, *w/v*). Next, transfer the tube into 65 °C water bath for 30 min to convert the N-formyl kynurenine to kynurenine. After centrifuged at 13.000 rpm for 10 min, the supernatant (100 μL) was transferred to a new 96-well microplate and an equal volume of freshly prepared 2% w/v *p*-dimethylaminobenzaldehyde in acetic acid was added. The optical density was measured at 480 nm using VarioskanFlash Multimode Reader (Thermo Fisher). The kynurenine concentration was determined from L-kynurenine standard curve.

2.6. IDO enzyme activity assay

The assay for the activity of recombinant expressed IDO1 was conducted as earlier described (Lin et al., 2016). In brief, the IDO activity was measured in a 50 mM potassium phosphate buffer (PBS, pH 6.5), where contains ascorbic acid (10 mM), methylene blue (10 μM), catalase (100 μg/mL), L-tryptophan (200 μM)), recombinant expressed IDO enzyme in 96-well black plates after incubating with the test compounds. NaOH was added and further incubated for the hydrolysis to kynurenine from N-formylkynurenine. The concentration of kynurenine formed was estimated by fluorescence emission (excitation 355 nm; emission 460 nm).

2.7. Determination of serum kynurenine

Serum kynurenine was determined by high-performance liquid chromatography (HPLC) as earlier described (Holmes, 1988). The chromatographic system was composed of HP 1050 series pump Hewlett-Packard, Rheodyne injection valve fitted with a sample loop (5 μL) and Waters Spherisorb S3 ODS2 150 × 2.1 mm column. Kynurenine concentrations measured according to Holms 1998. Using a HP 1050 series UV detector the column effluent was monitored at 365 nm. The mobile phase consisted of 0.1 M acetic acid, 0.1 M ammonium acetate (pH 4.65) containing 2% of acetonitrile and was pumped at a flow-rate of 0.25 mL/min.

2.8. Cell viability assay

The estimation of cell viability was carried out following an earlier protocol (Tominaga et al., 1999). Cells were treated with various concentrations of salinomycin in 100 μL of medium for 24 h. 10% of the Cell Counting Kit (CCK-8, Beyotime, Haimen, China) in 100 μL of fresh culture medium was added to each well, followed by incubation for 1 h with 5% CO_2 humidified incubator at 37 °C. Absorbance was measured at 450 nm by using a VarioskanFlash Multimode Reader (Thermo Fisher Scientific). Calculation of cell viability was estimated as a percentage of the control (DMSO, 0.5%).

2.9. Immunoblotting

The immunoblotting was conducted as described before (Kim, 2017). Cell lysis buffer (RIPA) supplemented with phenylmethylsulfonylfluoride (PMSF) (Sigma, Shanghai, China), was used to lyse the cells. Equal concentration of protein from various samples was loaded on the gel (10% sodium dodecyl sulfate-polyacrylamide) for electrophoresis. Afterward, the transfer of proteins to nitrocellulose membranes was followed by blocking for 1 h in a blocking buffer (5% bovine serum albumin, Tris-buffered saline, Tween 20). The various primary antibodies were used to incubate the membranes overnight at 4 °C. The next day incubation with an appropriate secondary antibody was followed by the visualization of bands in an enhanced chemiluminescence reagent (TransGen Biotech, Beijing, China) on ImageQuant LAS 500 (GE Healthcare Bio Sciences AB, USA).

2.10. Quantitative reverse transcription polymerase chain reaction (qRT-PCR)

The mRNA level of *IDO1* and *CYP1A1* was estimated following the qRT-PCR technique as described before (Rocha et al., 2016). The extraction of total cellular RNA was conducted with TRIzol reagent following the manufacturer's protocol (Life Technologies). Preparation of cDNA from total RNA (2 μg) was conducted with M-MLV reverse transcriptase and oligo (dt)15 primers (Promega). Equal amounts of cDNA (500 ng) were amplified by real-time quantitative PCR through using TransStart® Tip Green qPCR SuperMix kit (#AQ141, TransGen Biotech, Beijing, China) following the manufacturer's instructions. *IDO1* primers were as follows: forward 5′-TTCCTGGTCTCTCTATTGGTG-3′, reverse 5′-TAGCAAAGTGTCCCGTTCTT-3′; *CYP1A1* primers were as follows: forward 5′-CAAGAGGAGCTAGACACAGTGATT-3′ and reverse 5′-AGCCTTTCAAACTTGTGTCTCTTGT-3′ and glyceraldehyde-3-phosphate dehydrogenase (*GAPDH*) forward 5′-AGGTGAAGGTCGGAGTCA ACG-3′, reverse 5′-CCTGGAAGATGGTGATGGGAT-3′. PCR was carried out under the following conditions for *IDO1* and *CYP1A1*: Holding Stage at 94 °C for 30 s, followed by 45 cycles of 94 °C for 5 s and 60 °C for 30 s, and final with a Melt Curve Stage. Triplicate analyses of the samples were conducted and levels of *IDO1* and *CYP1A1* relative expression were normalized to that of *GAPDH* using the $2^{-\Delta\Delta Ct}$ method. The value of unstimulated cells was set at one and was used to calculate the fold change in stimulated cells.

2.11. Cellular thermal shift assay

The assay for the cellular thermal shift was carried out as previously described, with minor modifications (Jafari et al., 2014). Briefly, to induce the expression of IDO1 50 ng/mL IFN-γ was used to treat HeLa cells for 24 h. After cells harvest, PBS supplemented with the complete protease inhibitor cocktail was used for dilution. Cell suspensions were subjected to three rounds of freeze-thawing in a liquid nitrogen-water bath (37 °C). The cell lysate was centrifuged for 20 min at 20,000 ×*g* at a temperature of 4 °C. Thereafter, further dilution of cell supernatant with PBS was followed by dividing the cells into two aliquots; one aliquot was treated with DMSO and the other with 100 μM salinomycin. Aliquots were divided into 50 μL, followed by 30 min incubation at room temperature, and individual heating in a Fast-Thermal Cycler (Long Gene ®) at different temperatures (50–75 °C) at an interval of 3 min cooling period. After heating the lysates, 10 min centrifugation was conducted at 20,000 ×*g* in 4 °C and the soluble fractions were separated from the precipitates. The mixture of the supernatants and loading buffer were boiled for 5 min, and separated by SDS-PAGE, for western blotting analysis. The evaluation of the concentration-dependent impact of salinomycin on the IDO1 and vinculin stability was also estimated as described above.

2.12. Molecular docking model

Autodock 4 was used for molecular docking and the published IDO1 crystal structure (PDB code 4PK5) was employed as a source for the IDO1 structure (Yue et al., 2017). The preparation of IDO1 and salinomycin structures were conducted by adding hydrogen, deleting water, and removing disorder of the bond using AutoDock Tools. The

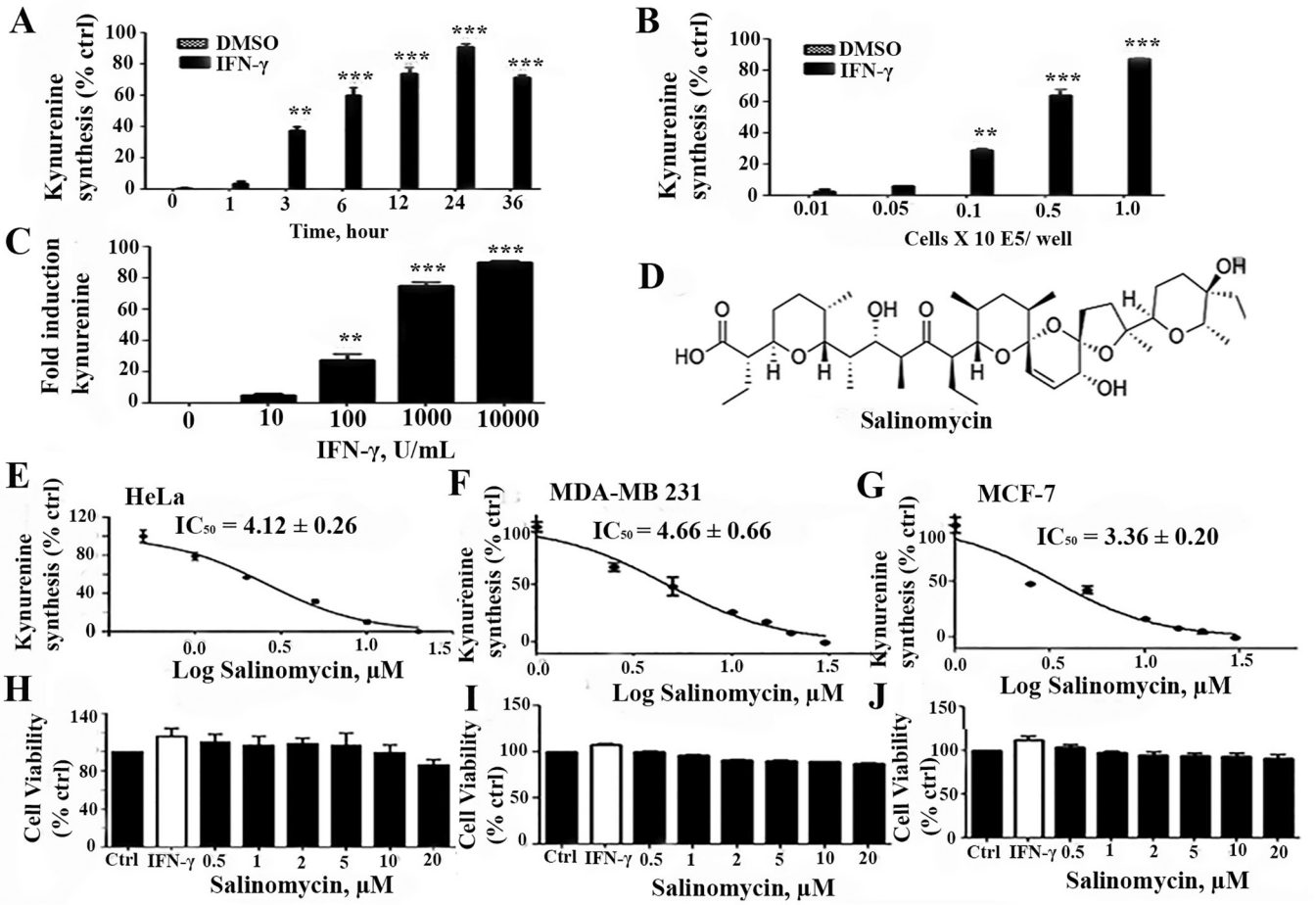

Fig. 1. Identification of salinomycin as an inhibitor of kynurenine synthesis. (**A**) HeLa cells seeded at a density 1×10^5 cells/well were incubated in DMSO or IFN-γ (50 ng/mL) in a time-dependent variation from 0 to 36 h. (**B**) The density of HeLa cells in 100 µL of DMEM varied from 0.01 to 1×10^5 cells/well in the 24 h incubation period. Thereafter, the substitution of the medium with 100 µL DMEM was done with or without IFN-γ. (**C**) IFN-γ stimulated kynurenine synthesis. HeLa cells were seeded in 100 µL DMEM for 24 h at a concentration of 1×10^5 cells/well. Thereafter, the medium was substituted with DMEM (100 µL) which contains a serial dilution of IFN-γ 0–10,000 U/mL for a further 24 h incubation period. (**D**) The chemical structure of salinomycin. **(E)**HeLa cells, **(F)** MDA-MB 231 cells, and **(G)** MCF-7 cells were pre-treated with different concentrations of salinomycin (0.5–20 µM) for 2 h, prior to the addition of IFN-γ (50 ng/mL). Cell supernatants were collected to measure the concentration of L-kynurenine. The calculated IC_{50} values were 4.13, 4.65, and 3.35 µM, respectively. The remaining cells were incubated in fresh medium containing 10% CCK-8. Cell viability was determined in HeLa cells (**H**), MDA-MB 231 cells **(I)**, and MCF-7 **(J)** and presented as percentage of the control (DMSO, 0.5%). The plot represents the average and standard deviations of the three experiments. $*p < 0.05$, $**p < 0.01$, $***p < 0.001$ significance difference relative to the control.

default parameters were used. The prediction of docking results was according to the energy of binding and the constant of inhibition. To obtain a population of potential conformations and orientations for salinomycin at the binding site, the default settings were used to perform the docking study.

2.13. Co-culture and T-cell proliferation assay

Female C57BL/6 mice aged 4–6 weeks were acclimatized for one week. The isolation of T cells from mouse spleen was by the method described by Flaherty and Reynolds (2015), with minor modifications. In brief, the spleens from freshly sacrificed mice were collected in a culture plate (60 mm) which contains PBS (3 mL). Thereafter, sterilized forceps were used to place a square of sterile nylon mesh over the tissue, followed by gently smashing the tissue against the mesh with the thumb side of a syringe plunger (3–10 mL). Thereafter, the remaining clumps which are soluble were dispersed by up and down pipetting for a few times. The remaining debris of splenic tissues was removed by placing a new square piece of nylon mesh over the opening of a 15 mL conical tube and filtered, following 5 min centrifugation at 475 ×*g* at 4 °C. Thereafter, the supernatant was discarded, and the cell pellets were resuspended in 1 mL of ice-cold 1× cell lysing solution per spleen for 1 min for erythrocyte lysis. A 10 mL volume of PBS was supplemented to the lysing solution. Subsequently, twice inversion of the tubes was followed by 5 min centrifugation at 475 ×*g* for 5 min at 4 °C. After centrifugation, the supernatant (splenocytes) was aspirated and resuspended in 10 mL of PBS. T cells from the splenocytes were purified using nylon wood fiber columns in accordance with the manufacturer's protocol (Polysciences, Warrington, PA, USA). All experiments with mice followed the regulations of Chinese Academy of Science guidelines for the care and use of Laboratory Animals and approved by the institutional animal care and use committee of Chengdu Institute of Biology, Chinese Academy of Science (protocol number: CIBCAS-2019-0139).

MDA-MB 231, MCF-7 and 4 T1 cells were co-cultured with isolated mouse T cells from mice. 100 µL of Cancer cells were co-cultured with 100 µL of mouse T cells at a density of 2×10^6 cells/ml into 96-well plates in a final volume of 200 µL for 48 h. After the co-culture period, the culture medium was discarded by pipetting, and cell viability was estimated using a CCK-8 counting kit as earlier described (Koyanagi et al., 2016; Ma et al., 2018). Naive T cells were isolated from the spleen of mice and pre-stained with 3 µM carboxyfluorescein diacetate

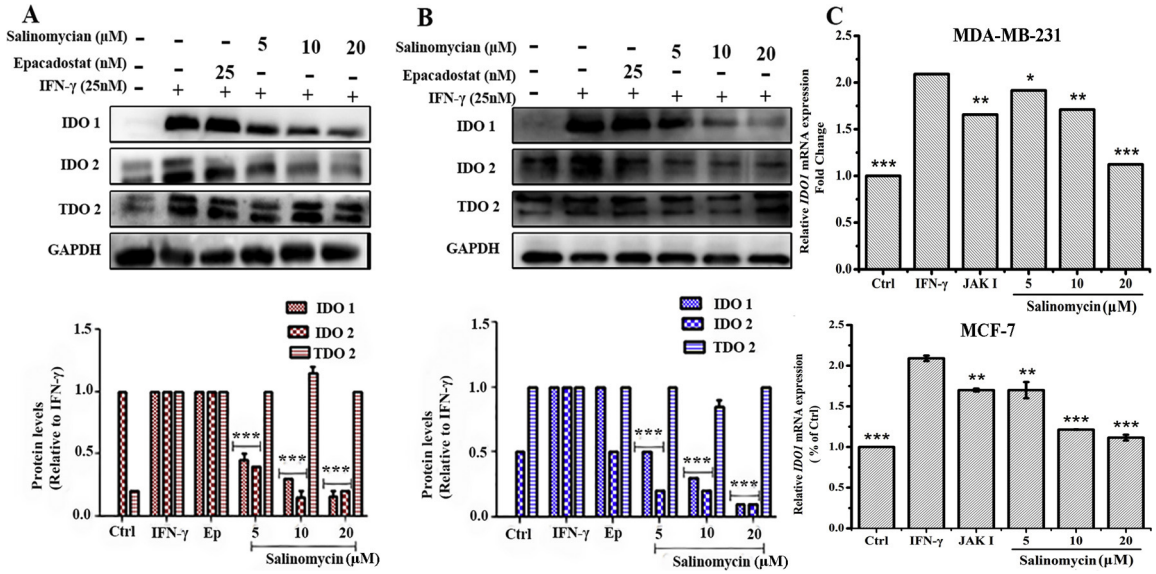

Fig. 2. Salinomycin inhibits the expression of IDO. **(A and B)** Before 24 h incubation of MDA-MB 231 and MCF-7 cells with 50 ng/mL IFN-γ, the cells were pre-treated for 2 h with salinomycin (5, 10, and 20 μM) and epacadostat (25 nM). Immunoblotting was conducted on cell lysates with the respective primary and secondary antibodies and detected via chemiluminescence. **(C)** Cells were pre-treated for 2 h with salinomycin (5, 10, and 20 μM) or JAK inhibitor I (1 μM) and 50 ng/mL IFN-γ was added for 12 h to stimulate IDO expression. Data represent mean ± standard error of mean (SEM) of three experiments; *$p < 0.05$, **$p < 0.01$, ***$p < 0.001$ compared with IFN-γ treatment alone.

succinimidyl ester (CFSE, Selleck Chemicals) at 37 °C for 15 min. The MDA-MB-231, MCF-7 and 4 T1 cells were stimulated with IFN-γ and co-cultured with the labeled T cells at a ratio of 1:5 (cancer cells: T cells) (Gao et al., 2019). The co-cultured cells were supplied with 100 ng/mL of anti-mouse CD3E antibody (Biolegend, San Diego, CA, USA) and 10 ng/mL of mouse recombinant interleukin (IL)-2 (Peprotech, Jersey, NJ, USA). After 3 days cocultured, the T cells proliferation was detected using FACS analysis (Qiao et al., 2019).

2.14. In vivo experiment

Female BALB/c mice aged 4–6 weeks were acclimatized for one week. After one-week acclimatization, 4 T1 cells were injected into the right flank of the breast fat pads of the mice at a density of 1×10^6 cells/100 μL/mouse. Tumor diameter was measured using a digimatic caliper and volume was calculated as ($a \times b^2$) where a, and b, were measured diameters in both dimensions. Mouse weight and tumor growth were monitored every other day. After 7 days of injecting 4 T1 cells, mice with tumor volume from 150 mm^3 and above were selected for the study, and randomly assigned into 4 groups ($n = 6$). Group 1 untreated mice. Group 2 received cisplatin (1 mg/kg). Group 3 received salinomycin (5 mg/kg). Group 4 received combination of cisplatin (1 mg/kg)and salinomycin (5 mg/kg). Doses of drugs were selected according to our preliminary study. Tumors were collected, and fixed in fixative solution. Embedded tissues were sectioned into 5–7 μm slices by rotary microtome. Immunohistochemistry (IHC) of tumor slices was performed using a primary antibody against IDO1. All experiments with mice followed the regulations of Chinese Academy of Science guidelines for the care and use of Laboratory Animals and approved by the Institutional Animal care and use committee of Chengdu Institute of Biology, Chinese Academy of Science (protocol number: CIBCAS-2020-004).

2.15. Statistical analyses

GraphPad Prism 5.0 software (GraphPad, La Jolla, CA, USA) was utilized for statistical analyses. All assays were conducted in triplicates, and result representatives are presented. Data comparison was conducted by one-way ANOVA, followed by Dunnett's post-hoc test. Data were considered statistically significant at $p < 0.05$.

3. Results

3.1. Cell-based screening of the inhibitors of kynurenine synthesis

To screen the natural products that could inhibit IFN-γ induced kynurenine synthesis, we utilized an in vitro assay with HeLa cell line treated with IFN-γ. To arrive at the conditions for the screening, we examined three variable parameters that influence the induction of the reaction, namely, time (period) of incubation, cell number variation, and IFN-γ concentration. Through optimization, we aimed to obtain the appropriate reactions and ensure the time efficiency of the screening. As shown in Fig. 1A, cells treated with IFN-γ could induce kynurenine synthesis after 1 h of exposure. This climaxed during 24 h and afterward began to decrease after 36 h, demonstrating that the ideal time point is 24 h for kynurenine activity in cells treated with the test compounds. Meanwhile, no induction was observed in cells treated with DMSO. To observe the consequence of cell density on kynurenine synthesis, different cell amounts were sub-cultured in a 96-well plate followed by IFN-γ treatment. The cell density of 1×10^5 cells/well showed higher activity response than $0.01–0.5 \times 10^5$ cells/well (Fig. 1B). Thus, as 1×10^5 cells/well elicited a higher activity, it was chosen for the screening experiment. To study the impact of the concentration of IFN-γ on kynurenine synthesis, cells were exposed to IFN-γ at different concentrations. As shown in Fig. 1C, concentration-dependent induction of kynurenine synthesis by IFN-γ was noticed in HeLa cells. Further, 1×10^3 and 1×10^4 U/mL IFN-γ increased kynurenine synthesis with a higher margin than the DMSO treatment, which caused no induction. These data indicate that cell density variations, time (period) of incubation, and concentration of IFN-γ significantly affect the performance of the assay. Therefore, HeLa cells were sub-cultured in 96-well plates at 1×10^5 cells/well, treated with a concentration of 1×10^3 U/mL IFN-γ, and incubation period of 24 h to evaluate kynurenine synthesis.

Under the conditions (1×10^5 cells/well in 96 well plate, 1×10^3 U/mL IFN-γ, and incubation period of 24 h, which represent the condition with highest activity), the screening was carried out in duplicate with a 10 μg/mL concentration of the purified compounds in

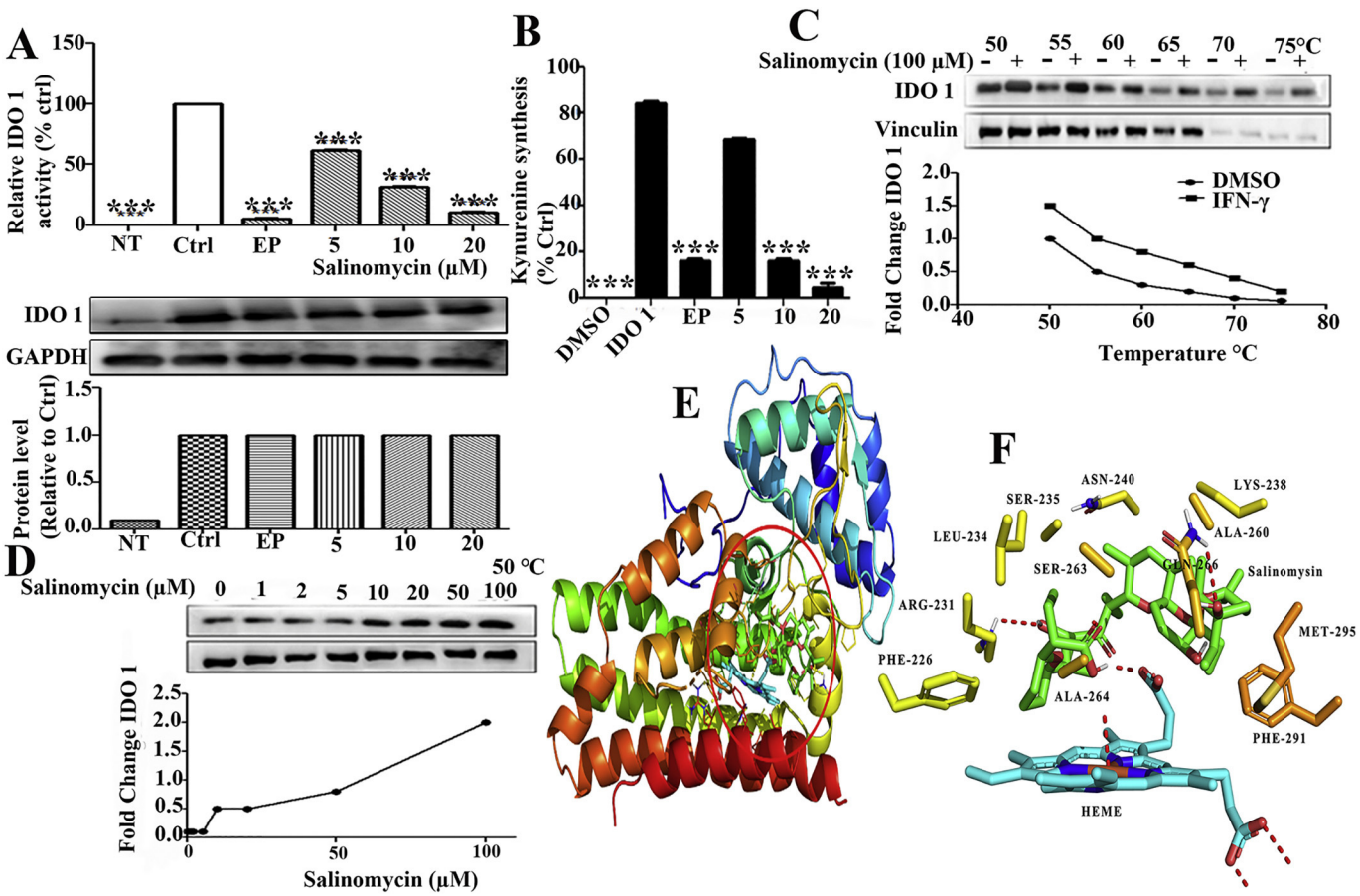

Fig. 3. Salinomycin inhibits IDO1 catalytic activity. **(A)** HEK293A cells were transfected with the pCMV3-IDO1 plasmid and incubated for 48 h. After that cells were treated with salinomycin (5, 10, and 20 μM) or epacadostat (25 nM) for 2 h. Thereafter, the cell supernatants were used to measure IDO1 activity, and the cell lysates were immunblotted with anti-IDO1 antibody. GAPDH was employed as the loading control. (**B**) The catalytic activity of the recombinant expressed IDO1 protein was measured. (**C, D**) IFN-γ-stimulated HeLa cells were subjected to cellular thermal shift assay. The impact of salinomycin in stabilizing IDO1 and vinculin under various temperatures **(C)** or various concentrations of IFN-γ **(D)** was evaluated by western blot. (**E**) Molecular docking of the IDO1 protein and salinomycin. **(F)** Stereoview of the active site of the IDO1–salinomycin complex. Data represent mean ± standard error of mean (SEM) of three experiments; $^{**}p < 0.01$, $^{***}p < 0.001$ compared with the control.

a chemical library containing 1431 natural products and their synthetic analogs (Tai et al., 2012). After primary (screening of the whole 1431 compounds) and confirmatory screening (re-screening of the compounds with inhibitory effects > 30%), salinomycin was selected for further studies. The chemical structure of salinomycin is presented in Fig. 1D. To determine the impact of salinomycin owing to IFN-γ stimulation on kynurenine synthesis, different concentrations of salinomycin from 0.5 to 20 μM were administered to cells (HeLa, MDA-MB 231, and MCF-7) for 2 h followed by 24 h incubation with IFN-γ. As shown in Fig. 1E, F, and G, salinomycin concentration-dependently inhibited kynurenine synthesis with IC_{50} values of 4.13, 4.65, and 3.36 μM, respectively, in HeLa, MDA-MB 231, and MCF-7 cells. Additionally, salinomycin elicited no significant impact on the reduction of cell viability at the tested concentrations, despite the slight decrease in cell viability at 20 μM as depicted in Fig. 1H, I, and J. Our results suggest that salinomycin is a potent inhibitor of kynurenine synthesis without affecting cell viability at the tested concentrations.

3.2. Salinomycin inhibits the expression of IDO

Three enzymes, namely, IDO1, IDO2, and TDO, are involved in the catalysis of tryptophan degradation into kynurenine. To identify the enzyme responsible for salinomycin inhibition of kynurenine synthesis, we evaluated the effect of salinomycin on these proteins. As shown in Fig. 2A and B, salinomycin suppressed the expression of IDO1 and IDO2 but did not affect TDO2 in both cells (MDA-MB 231 and MCF-7). Salinomycin also inhibited the kynurenine synthesis and IDO1 expression in 4 T1 cells (Fig. S1). IDO1 expression was notably stimulated after treatment with IFN-γ, which was significantly repressed in a concentration-dependent manner by salinomycin. Concomitantly, IDO2, which is constitutively expressed in cells, was also inhibited at all tested concentrations. By analyzing the effect of salinomycin on IDO1 expression at the transcriptional level, we observed a dose-dependent lower expression of *IDO1* mRNA level following pre-treatment with salinomycin in both cells than that by IFN-γ treatment alone (Fig. 2C). These findings suggest that salinomycin exerts its inhibitory effect on *IDO1* expression at the transcriptional level.

3.3. Salinomycin inhibits the enzymatic activity of IDO1

To examine the inhibitory effect of salinomycin on the enzymatic activity of IDO1, IDO2 and TDO2, we transfected HEK 293A cells with the pCMV3-IDO1, IDO2 and TDO2 plasmids. Thereafter, the transfected cells were treated for 2 h with salinomycin (5, 10, and 20 μM). As shown in Fig. 3A and Fig. S3, salinomycin significantly inhibited IDO1 and IDO2 catalytic activity in a concentration-dependent manner similar to epacadostat, a known IDO1 inhibitor, without affecting the catalytic activity of TDO2. Also, salinomycin significantly repressed the enzymatic activity of recombinant expressed IDO1 protein in a dose-dependent manner (Fig. 3B). To examine whether salinomycin directly

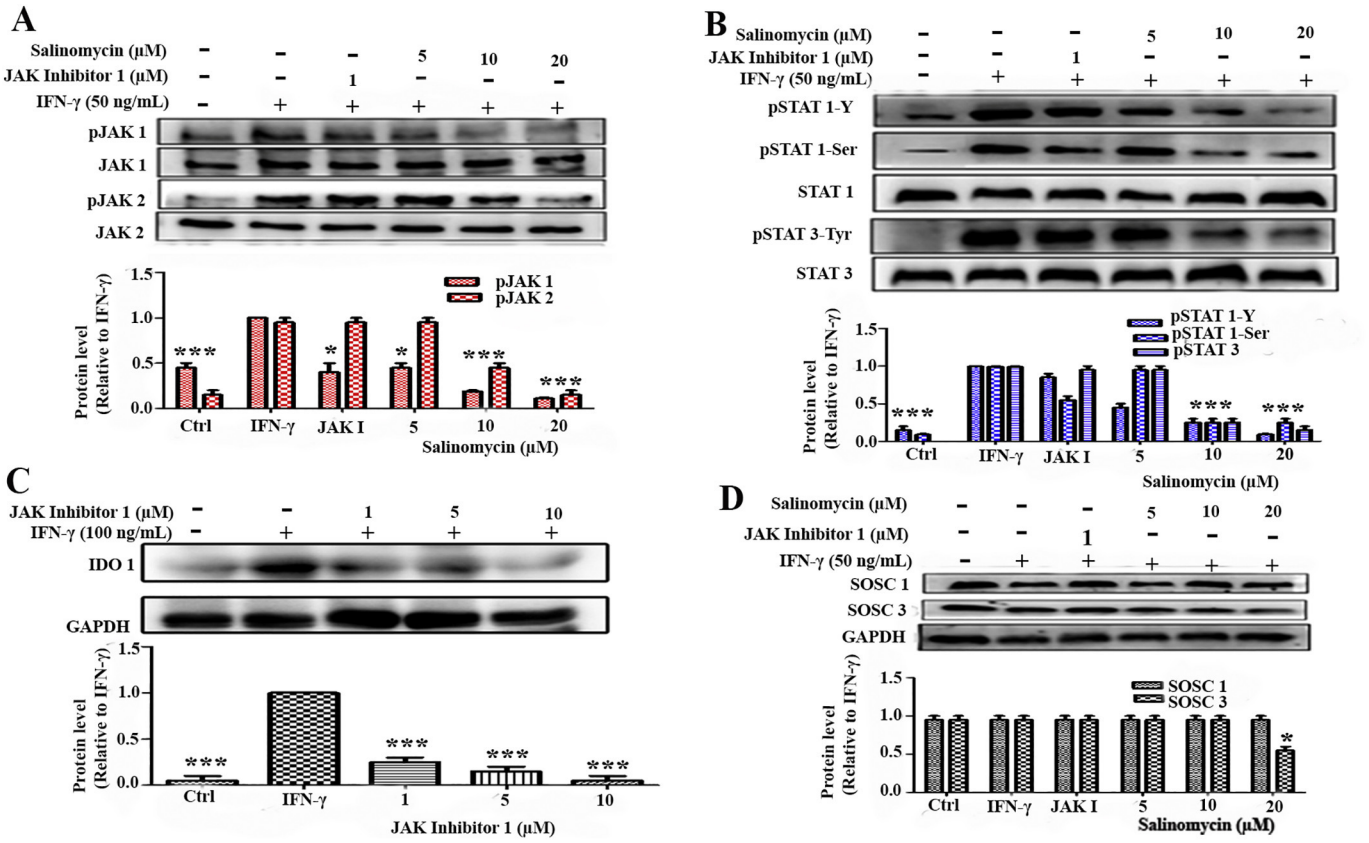

Fig. 4. Salinomycin inhibits the activation of the JAK/STAT pathway. Prior to the addition of INF-γ (50 ng/mL) to MDA-MB 231 cells for 30 min, the cells were treated with salinomycin (5, 10, 20 μM) and JAK inhibitor I (1 μM) for 2 h. Thereafter, immunoblotting of the cell lysates was analyzed with anti-phospho-JAK1 (Tyr1022), anti-JAK1, anti-phospho-JAK2 (Y1007/1008), anti-JAK2 (**A**), anti-phospho-STAT1 (Y701), anti-phospho-STAT1 (Ser727), anti-STAT1, anti-phospho-STAT3 (Tyr705), and anti-STAT3 antibodies, respectively (**B**). **(C)** Prior to the addition of IFN-γ (100 ng/mL) to MDA-MB 231 cells for 24 h, the cells were treated for 2 h with JAK inhibitor I (1, 5, and 10 μM). Thereafter, immunoblotting of the cell lysates with the anti-IDO1 antibody was conducted. The loading control was GAPDH. (**D**) IFN-γ (50 ng/mL) was added to MDA-MB 231 cells followed by 24 h incubation, and treated with salinomycin (5, 10, and 20 μM) and JAK inhibitor I (1 μM) for 24 h. Thereafter, immunoblotting of the cell lysates with anti-SOCS1 and anti-SOCS3 antibodies was analyzed. The loading control was GAPDH. Data represent mean ± standard error of mean (SEM) of three experiments; $^{**}p < 0.01$, $^{***}p < 0.001$ vs. the control.

interacts with IDO1 in cells, we applied cellular thermal shift assay, a recently established technique to estimate the binding of drugs to target protein in cells (Jafari et al., 2014). Compared to the control (DMSO), the treatment with salinomycin resulted in significantly higher IDO1 accumulation at the observed temperatures in the soluble fraction of cells (Fig. 3C). An increase in salinomycin concentration caused a marked increase in IDO1 accumulation (Fig. 3D). These findings further suggest that salinomycin is a potent inhibitor of IDO1 in cancer cells. A molecular docking experiment was used to analyze the potential binding modes of salinomycin with IDO1. Salinomycin aligned well in the IDO1 active site with a binding energy of -6.94 kcal mol^{-1} (Fig. 3E). The formation of hydrogen bonding and hydrophobic interactions between salinomycin and IDO1 were evaluated to determine the modes of binding of salinomycin with IDO1. As shown in Fig. 3F and Fig. S4, salinomycin and IDO1 formed three hydrogen bonds to maintain the binding stability. These bonds were formed with the three residues, Arg-231, Ala-264, and Gln-266, and the hydrogen-forming residue, Ala-264, also formed a hydrogen bond with heme. Salinomycin could also combine with other residues, such as Phe-291, Met-295, Ala-260, Lys-238, Asn-240, Ser-235, Leu-234, and Phe-226, via a hydrophobic force. These data suggest that salinomycin prompted an alignment that favors a nucleophilic attack in the active site of IDO1.

3.4. Salinomycin inhibits the activation of the JAK/STAT pathway

IDO1 expression can be activated in most human cells by several mediators, including INF-γ, which activate the transcription of *IDO1* through the JAK/STAT pathway. Thus, we theorized that the decrease of IDO1 expression might occur via the downregulation of this signaling pathway. First, we assessed the impact of salinomycin on the IFN-γ instigated JAK/STAT signaling pathway. As shown in Fig. 4A, salinomycin significantly decreased the phosphorylation of tyrosine JAK1 and JAK2 in a dose reliant manner. Consistently, salinomycin significantly diminished the STAT1 and STAT3 phosphorylation in a dose reliant manner (Fig. 4B). To confirm the vital role of the JAK/STAT pathway in the control of IDO1 expression, we analyzed the impact of the JAK inhibitor on IDO1 protein expression. As shown in Fig. 4C, the JAK inhibitor abolished the stimulatory effect of IFN-γ on IDO1 expression. Further, by examining the influence of salinomycin on the expression of SOCS1 and SOCS3, the negative regulators of the JAK/STAT pathway, we observed that salinomycin had no impact on SOCS1 expression but decreased SOCS3 eccxpression at 20 μM (Fig. 4D). These results suggest that salinomycin decreased IFN-γ-induced IDO1 expression by inhibiting the JAK/STAT pathway.

3.5. Salinomycin inhibits the activation of the NF-κB pathway

NF-κB pathway has been implicated in the regulation of IDO1 expression. Thus, we further examined the impact of salinomycin on this pathway. As shown in Fig. 5A, salinomycin significantly blocked the degradation of IκBα and phosphorylation of NF-κB, without any impact on the total expression of NF-κB. To ascertain the implication of the NF-

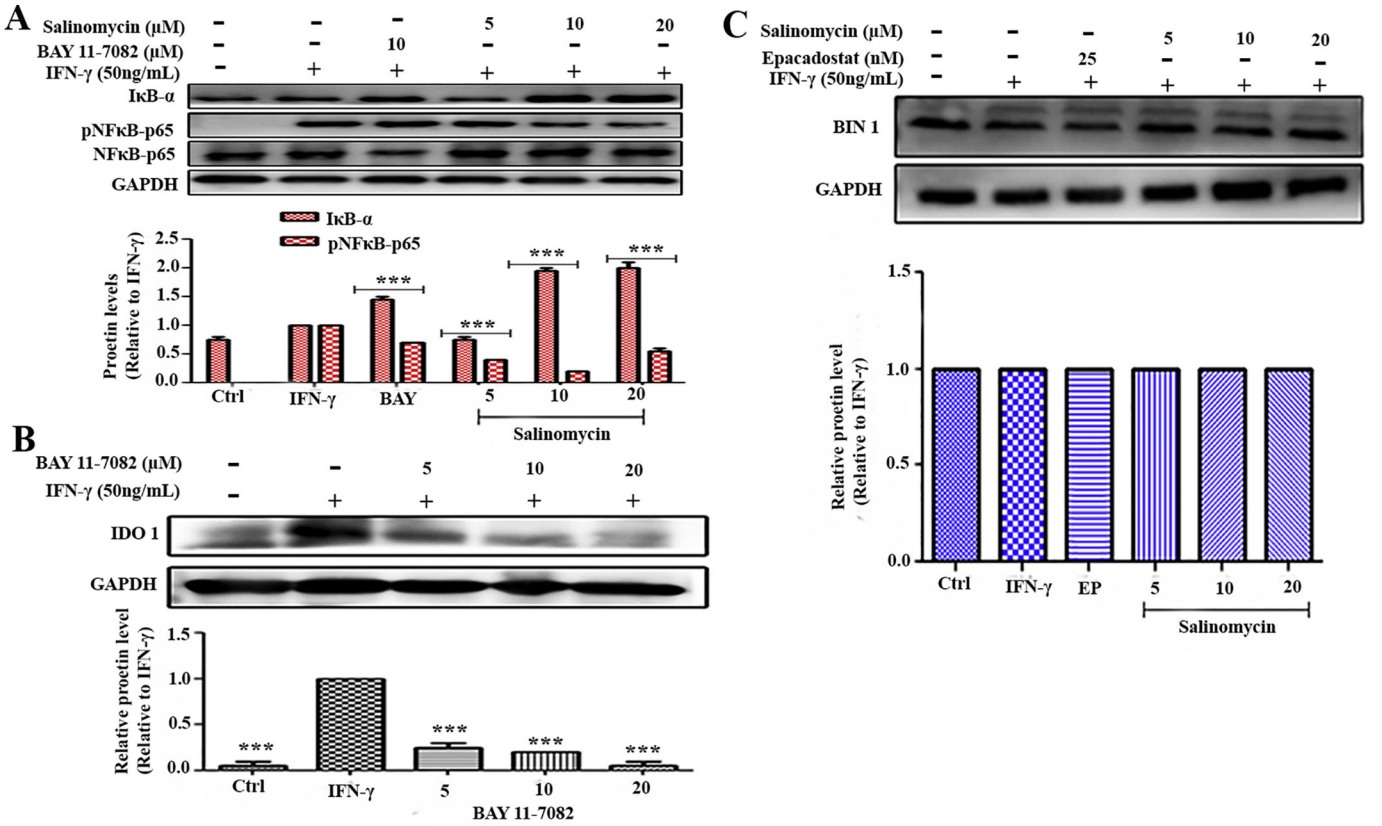

Fig. 5. Salinomycin inhibits the activation of the NF-κB pathway. (**A**) Prior to the addition of 50 ng/mL of INF-γ to MDA-MB 231 cells for 30 min, the cells were treated with salinomycin (5, 10, and 20 μM) and BAY11–7082 (10 μM) for 2 h. Thereafter, the cell lysates were immunoblotted with the anti-IκBα, anti-phospho-NF-κB-p65 (Ser 536), anti-NF-κB-p65 antibodies, respectively. (**B**) MDA-MB 231 cells were treated with BAY11–7082 (5, 10, and 20 μM) for 2 h before the addition of IFN-γ (100 ng/mL) for 24 h. Cell lysates were immunoblotted with the anti-IDO1 antibody. GAPDH was employed as the loading control. (**C**) Prior to the addition of 50 ng/mL IFN-γ to MDA-MB 231 cells for 24 h, the cells were treated with salinomycin (5, 10, and 20 μM) and epacadostat for 2 h. Thereafter, the cell lysates were immunoblotted with the anti-BIN1 antibody. GAPDH was employed as the loading control. Data represent mean ± standard error of mean (SEM) of three experiments; $^{**}p < 0.01$, $^{***}p < 0.001$ vs. the control.

κB pathway in the regulation of IDO1 expression, we examined the effect of BAY11–7082 (NF-κB inhibitor) on IDO1 protein expression. As shown in Fig. 5B, BAY11–7082 repealed IFN-γ stimulatory effect on IDO1 expression. Furthermore, by analyzing the effect of salinomycin on the expression of BIN1, a tumor suppressor that controls the expression of IDO1 (Muller et al., 2005), we found that salinomycin did not alter BIN1 expression as shown in Fig. 5C. We then examined the effect of salinomyicin on the expression of cytochrome P450 1A1 (*CYP1A1*), a biomarker for aryl hydrocarbon receptor (AhR) activation that upregulates IDO1 expression in cells (Vogel et al., 2008). StemRegenin-1(SRI), an antagonist of AhR, significantly decreased IFNγ-induced *CYP1A1* expression whereas salinomycin had no effect (Fig. S5). These results suggest that the decrease in IFN-γ-induced IDO1 expression by inhibiting the NF-κB pathway but not BIN1 and AhR pathways.

3.6. Effects of salinomycin on T-cell viability

To determine the potential influence of salinomycin treatment on T-cell proliferation, T cells were isolated from spleen of mice and co-cultured with breast cancer cells (human MDA MB-231, MCF-7, and mouse 4 T1 cells). As shown in Fig. 6, treatment with IFN-γ suppressed the proliferation of co-cultured cells in MDA-MB 231, MCF-7, and 4 T1 cell whereas treatment with salinomycin significantly restored the proliferation of the T cells. This finding indicates that suppression of IFN-γ-induced IDO expression owing to salinomycin treatment in cancer cells could enhance T-cell proliferation.

3.7. In vivo antitumor activity of salinomycin

To investigate whether salinomycin potentiates cancer chemotherapy as IDO1 inhibitiors did (Muller et al., 2005), we used a 4 T1 murine breast cancer xenograft mouse model. The combination treatment of salinomycin and cisplatin significantly suppressed the tumor growth compared to individual cisplatin or salinomycin treatment (Fig. 7A-C). Salinomycin had no effect on body weight within the treatment period (Fig. S6). Furthermore, there was a significant decrease in kynurenine concentration in serum or tumor from the mice treated with salinomycin and in combination with cisplatin treatment groups (Fig. 7D and E). The expression of IDO1 in 4 T1 tumor tissues was evaluated by immunohistochemistry (IHC). As shown in Fig. S7, salinomycin treatment alone or the combination treatment of cisplatin plus salinomycin decreased the IDO1 expression in tumor tissues compared with the control group. In addition, we observed an increase in the number of tumor-infiltrating $CD8^+$ T cells treated with salinomycin compared to the control group (Fig. S8). Taken together, these data suggest that salinomycin potentiated antitumor activity of cisplatin through inhibition of IDO1 and increase of accumulation and infiltration of T cells in vivo.

4. Discussion

Breast cancer is the most recurrently diagnosed cancer and the leading cause of cancer deaths worldwide among women (Torre et al., 2017; Yang et al., 2019a). The elevated IDO1 expression in tumor cells and tumor-draining lymph nodes correlate with tumor progression and

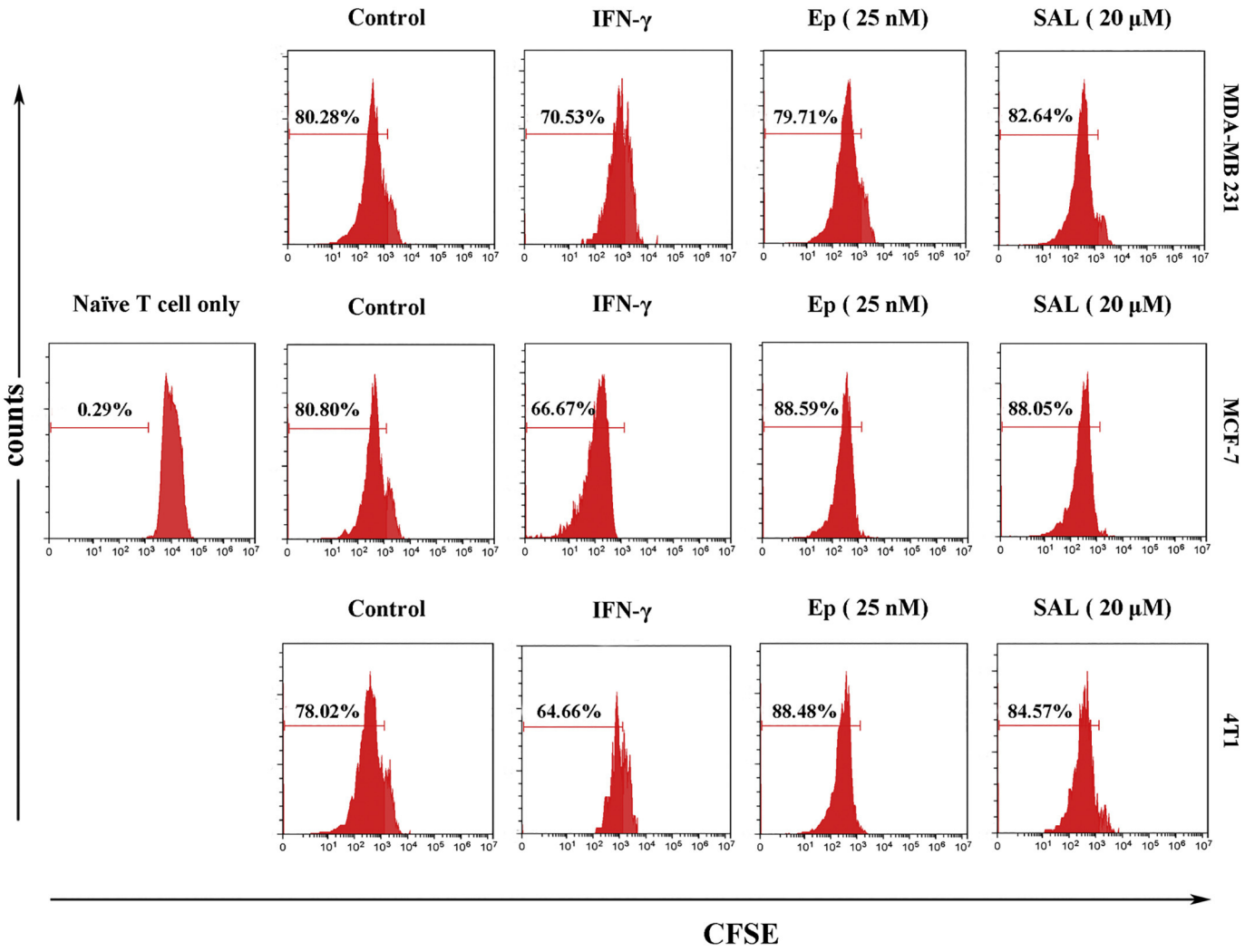

Fig. 6. Effect of salinomycin on T-cell viability. **(A)** Effects of salinomycin treatment on the viability of T cells co-cultured with human IFN-γ-treated MDA-MB 231 cells, MCF-7 cells and 4 T1 cells Cell proliferation was examined based on CFSE dilution using FACS. The percentage of proliferating cells is shown.

the adverse clinico-pathological conditions of patients (Godin-Ethier et al., 2011). Thus, IDO1 might serve as a target in breast cancer immunotherapy (Soliman et al., 2013). Our findings demonstrate that salinomycin is a potent inhibitor of IDO1 activity. Further, we demonstrated that it downregulates both IDO1 and IDO2 without any effect on TDO2 expression in human breast cancer cells. As IDO1, IDO2, and TDO2 differ in their quaternary structures, their expression and regulation in normal versus transformed tissues are quite distinct (Pilotte et al., 2012). IDO1 mediates the breakdown of both D- and L-tryptophan while TDO2 is specifically active on L-tryptophan (Zhai et al., 2015). The failure of epacadostat in phase III clinical trial was attributed to its specific inhibition of the enzymatic activity of IDO1, whereas IDO2 or TDO may compensate for kynurenine synthesis (Günther et al., 2019). As a result, the discovery of compounds with the potential to simultaneously inhibit IDO activity/expression is more preferred. Herein, we found that salinomycin not only decreased the expression of IDO1 and IDO2 but also inhibited their enzymatic activity, adding to its value in the development of a new dual-functional IDO pathway inhibitor for cancer immunotherapy. IDO1 and IDO2 share approximately 43% structural similarity at the amino acid level relative to the TDO2 protein sequence, which is not homologous to the IDO enzymes (Bakmiwewa et al., 2012). Thus, the inhibitory effect of salinomycin on the enzymatic activity of IDO1 and IDO2 should be further evaluated. Earlier studies have shown that salinomycin selectively eradicates apoptosis-resistant cancer cells and cancer stems cells (Gupta et al., 2009; Mai et al., 2017). However, the immune modulatory effect of salinomycin has not been addressed. In this study we found that salinomycin inhibits the enzymatic activity and expression of immunosuppressive IDO1 and IDO2, thereby providing new insights into the potential of salinomycin to reduce tumor growth by modulating IDO activity/expression in the tumor microenvironment.

Although the anticancer mechanism of salinomycin is yet to be fully identified, several studies demonstrated inhibitory impact of salinomycin against tumor growth by interfering with Akt signaling, Wnt/β-catenin, Hedgehog, and Notch pathways (Naujokat and Steinhart, 2012; Dewangan et al., 2017). Salinomycin also inhibits STAT3 activation in ovarian, gastric, and breast cancer cells (An et al., 2015; Koo et al., 2013; Mao et al., 2014). However, it is still unknown whether it interferes with the stimulation of JAK/STAT pathway by IFN-γ. In the current study, the IFN-γ induced phosphorylation of JAK1 and JAK2, which in tandem increased the phosphorylation of STAT1 and STAT3, was significantly suppressed in salinomycin pretreated MDA-MB 231 cells. Both STAT1 and STAT3 were found to regulate the transcription of *IDO1* (Sotero-Esteva et al., 2000; He et al., 2010; Yu et al., 2014). Our findings further confirm the inhibitory influence of salinomycin on the expression of IDO1, which may occur via the blockage of the JAK-STAT signaling pathway. This is consistent with the reports from earlier studies in which the JAK/STAT pathway was shown to be implicated in the regulation of IDO expression (Zhang et al., 2013; Luo et al., 2018). As a negative regulator of the JAK/STAT pathway, SOCS3 drives the

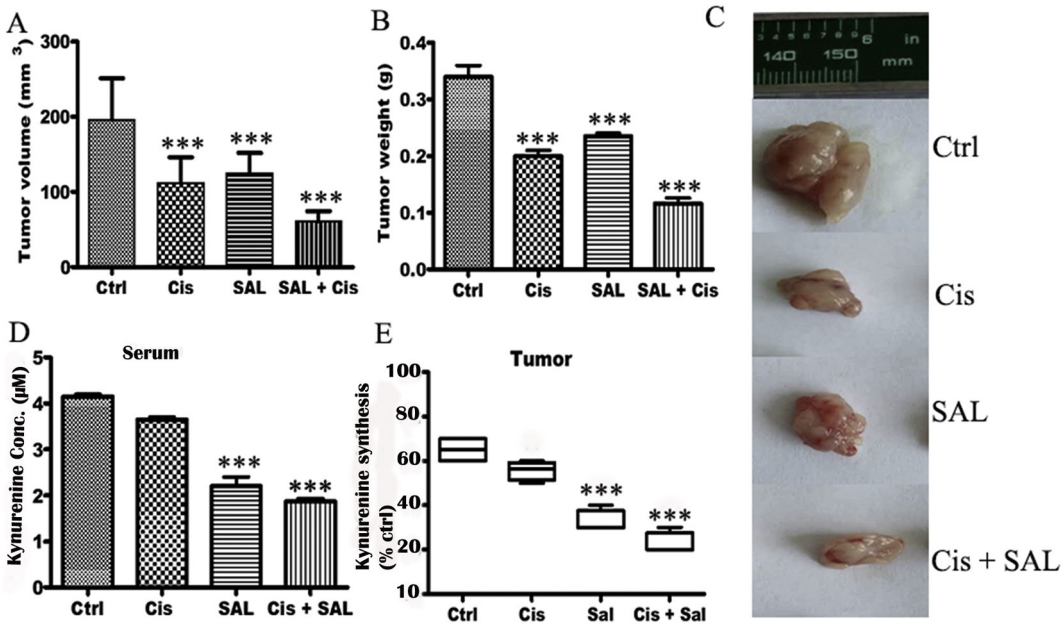

Fig. 7. Salinomycin potentiates antitumor activity of cisplatin. **(A)** Tumor volume of all the treatment groups. **(B)** Tumor weights in all the treatment groups. **(C)** Image of the representative tumors in the treatment groups. **(D)** Serum kynurenine concentration in the treatment groups. **(E)** Tumor kynurenine concentration in the treatment groups. Ctrl (untreated), Cis (1 mg/kg cisplatin), SAL (5 mg/kg salinomycin), Cis + SAL (1 mg/kg cisplatin +5 mg/kg salinomycin). ***p < 0.001 vs. the control (n = 6).

proteasomal degradation of IDO and antagonizes IDO-dependent tolerogenesis (Orabona et al., 2008). Our findings revealed that salinomycin slightly decreased the expression of SOCS3, excluding its potential to increase SOCS3 to inhibit JAK/STAT activation and promote IDO degradation. Myeloid-derived suppressor cells mediate immunosuppression in breast cancer cells via the activation of NF-κB which in turn aggravates STAT3-stimulated IDO upregulation in breast cancer cells (Yu et al., 2014). In the present study, IFN-γ treatment activated the NF-κB pathway in breast cancer cells by degrading IκB-α and phosphorylating NFκB-p65, which were evidently inhibited by salinomycin pretreatment. These findings suggest the implication of NF-κB pathway in the suppression of IDO expression/activity in breast cancer cells owing to salinomycin treatment. Salinomycin targets prostate and ovarian cancer cells by inhibiting the NF-κB pathway (Ketola et al., 2012; Parajuli et al., 2013), implying that salinomycin may exert its anticancer effect by inhibiting NF-κB-mediated IDO expression. AhR overexpression is associated with activation of NF-κB activity and upregulation of inflammatory markers like IL-6 secretion, leading to increase IDO activity/expression which is critical for cancer initiation (Vogel et al., 2008; Xue et al., 2018). However, some of IDO1 inhibitors were found to activate the AhR (Moyer et al., 2017). In our study, we found that salinomycin had no effect on CYP1A1 gene expression in MDA MB-231 cells. This precludes the possibility of the involvement of AhR pathway in its regulation of IDO1, which is supported by our finding that salinomycin decreased IDO1 or IDO2 expression whereas AhR activation promotes IDO1 or IDO2 expression (Vogel et al., 2008). However, further studies are needed to evaluate the effect of salinomycin on canonical and non-canonical AhR signaling pathways (Wright et al., 2017).

Although salinomycin exhibited potent activity against cancer stem cells, its cytotoxic effects on cancer cells are not substantial in vivo. Therefore, to enhance its activity in cancer stem cells and cancer cells in vivo, salinomycin is loaded into nanoparticles (Li et al., 2017; Daman et al., 2018; Zhao et al., 2019). Ironomycin, a synthetic derivative of salinomycin, shows a better effective and selective activity to counter breast cancer stem cells in vitro and in vivo. It sequesters iron in lysosomes and triggers a cell death pathway in a manner similar to ferroptosis (Mai et al., 2017). Interestingly, salinomycin instigated apoptotic death in human T cells of leukemia, thereby leaving normal human T lymphocytes unharmed (Fuchs et al., 2009). Additionally, salinomycin induces apoptosis of human colorectal cancer cells with attendant accumulation of dysfunctional mitochondria and reactive oxygen species, which are associated with expressional down-regulation of superoxide dismutase-1 (Klose et al., 2019). To date, however, its effect on cancer immunotherapy remains unclear. The increased expression of IDO was implicated in cancer progression via the blockage of T-cell activation, which caused T-cell death (Bourgeois et al., 2018). Thus, an anticancer therapy that targets this enzyme is warranted (Munn and Mellor, 2007; Johnson and Munn, 2012). Herein, salinomycin reversed the inhibitory impact of IFN-γ on the proliferation of primary T cells co-cultured with breast cancer cells, thereby aligning with our finding that salinomycin decreases IFN-γ-stimulated L-kynurenine concentration by inhibiting IDO1 expression and enzymatic activity in vitro and in vivo. Numerous preclinical cancer models indicate that single-agent regimen with an IDO1 inhibitor is only slightly effective. It has been inferred that reversion of recognized tumors can be accomplished by combination therapy of a cytotoxic chemotherapeutic drug with an IDO inhibitor (Muller and Prendergast, 2005). Consistent with that, here we found that combination of salinomycin and cisplatin elicited higher antitumor efficacy with the suppression of kynurenine synthesis and IDO1 expression in vivo. This also aligns with the observation that salinomycin ameliorates toxicity and exhibits synergistic effects when combined with many chemotherapeutic drugs (Dewangan et al., 2017). Immunotherapy exerts anticancer effects by activating competent immune effectors, such as T cells, and inhibiting immunosuppressive cells, such as myeloid-derived suppressor cells (Bourgeois et al., 2018). Salinomycin may exert its anticancer effect by modulating immune response in addition to its direct inhibition of cancer stem cells and cancer cells. Clinical pilot studies revealed that intravenous administration of salinomycin elicited incomplete clinical regression of heavily pretreated and therapy-resistant breast and vulvar carcinoma cancers with minor side effects, particularly when combined with novel tumor-targeting drugs (Naujokat and Steinhart, 2012). Our findings, which implicate that salinomycin is a novel immunotherapeutic agent owing to its inhibition of IDO, provide new insights into the anticancer mechanism of salinomycin and reveal the

approach required for drug delivery, dose optimization, and amelioration of systemic toxicity in future clinical studies.

In summary, by screening a natural product-based library, salinomycin was identified as a potent inhibitor of kynurenine synthesis as it could decrease the expression of both IDO1 and IDO2. In addition to directly inhibiting the enzymatic activity of the IDO protein, salinomycin inhibited the expression of IDO in breast cancer cells by downregulating the JAK/STAT and NF-κB pathways, reversing IFN-γ-induced suppression of T-cell proliferation and potentiating antitumor activity of cisplatin in vivo. These results provide new insights into the anticancer effects of salinomycin and indicate the need for its further development as a novel dual-functional IDO inhibitor for cancer immunotherapy.

Author contributions

F.W., L.L., X.X.L., G.L.Z., A.A.H conceived the experiments. A.P.E., E.M.N., Y.W.S., Z.H.Z., L.S., Z.Y.Z., Z.Q. and P.T. conducted the experiments. F.W., L.L., and A.P.E. analyzed the data and wrote the paper.

Declaration of Competing Interest

The authors have no conflict of interest to declare.

Acknowledgments

This work was supported by the National Natural Science Foundation of China (Nos. 21861142007, 21672207), Chinese Academy of Sciences President's International Fellowship Initiative (Nos. 2018 PB0017, 2015 PB049), Science & Technology Department of Sichuan Province (No. 2016JZ0022), Biological Resources Programme, Chinese Academy of Sciences (KFJ-BRP-008), and the National New Drug Innovation Major Project of China (2018ZX09711001-001-006).

Appendix A. Supplementary data

Supplementary data to this article can be found online at https://doi.org/10.1016/j.taap.2020.115203.

References

An, H., Kim, J.Y., Oh, E., Lee, N., Cho, Y., Seo, J.H., 2015. Salinomycin promotes anoikis and decreases the CD44+/CD24- stem-like population via inhibition of STAT3 activation in MDA-MB- 231 cells. PLoS One 10, e0141919.
Bakmiwewa, S.M., Fatokun, A.A., Tran, A., Payne, R.J., Hunt, N.H., Ball, H.J., 2012. Identification of selective inhibitors of indoleamine 2,3-dioxygenase 2. Bioorg. Med. Chem. Lett. 22, 7641–7646.
Bourgeois, T.L., Strauss, L., Aksoylar, H.-I., Daneshmandi, S., Seth, P., Patsoukis, N., Boussiotis, V.A., 2018. Targeting T cell metabolism for improvement of cancer immunotherapy. Front. Oncol. 8, 237.
Daman, Z., Faghihi, H., Montazeri, H., 2018. Salinomycin nanoparticles interfere with tumor cell growth and the tumor microenvironment in an orthotopic model of pancreatic cancer. Drug Dev. Ind. Pharm. 44, 1434–1442.
Dewangan, J., Srivastava, S., Rath, S.K., 2017. Salinomycin: a new paradigm in cancer therapy. Tumor Biol. 17, 1–12.
Dill, E.A., Dillon, P.M., Bullock, T.N., Mills, A.M., 2018. IDO expression in breast cancer: an assessment of 281 primary and metastatic cases with comparison to PD-L1. Mod. Pathol. 31, 1513–1522.
Flaherty, S., Reynolds, J.M., 2015. Mouse naïve CD4+ T cell isolation and in vitro differentiation into T cell subsets. J. Vis. Exp. 98, e52739.
Fuchs, D., Heinold, A., Opelz, G., Daniel, V., Naujokat, C., 2009. Salinomycin induces apoptosis and overcomes apoptosis resistance in human cancer cells. Biochem. Biophys. Res. Commun. 390, 743–749.
Gao, J., Deng, F.S., Jia, W.D., 2019. Inhibition of indoleamine 2,3-dioxygenase enhances the therapeutic efficacy of immunogenic chemotherapeutics in breast cancer. J. Breast Cancer 22, 196–209.
Godin-Ethier, J., Hanafi, L.A., Piccirillo, C.A., Lapointe, R., 2011. Indoleamine 2,3-dioxygenase expression in human cancers: clinical and immunologic perspectives. Clin. Cancer Res. 17, 6985–6991.
Günther, J., Däbritz, J., Wirthgen, E., 2019. Limitations and off-target effects of tryptophan-related IDO inhibitors in cancer treatment. Front. Immunol. 10, 1801.
Gupta, P.B., Onder, T.T., Jiang, G., Tao, K., Kuperwasser, C., 2009. Identification of selective inhibitors of cancer stem cells by high-throughput screening. Cell. 138, 645–659.
Hamid, O., Bauer, T.M., Spira, A.I., Smith, D.C., Olszanski, A.J., Tarhini, A.A., 2017. Safety of epacadostat 100 mg bid plus pembrolizumab 200 mg Q3W in advanced solid tumors: phase 2 data from ECHO-202/KEYNOTE-037. J Clin Oncol. 35 (Suppl) 3012. 42.
He, X.-S., Nanda, S., Ji, X., Calderon-Rodriguez, G.M., Greenberg, H.B., Liang, T.J., 2010. Differential transcriptional responses to interferon-α and interferon-γ in primary human hepatocytes. J. Interf. Cytokine Res. 30, 311–320.
He, L., Wang, F., Dai, W.Q., Wu, D., Lin, C.L., Wu, S.M., Cheng, P., Zhang, Y., Shen, M., Wang, C.F., Lu, J., Zhou, Y.Q., Xu, X.F., Xu, L., Guo, C.Y., 2013. Mechanism of action of salinomycin on growth and migration in pancreatic cancer cell lines. Pancreatology. 13, 72–78.
Holmes, E.W., 1988. Determination of serum kynurenine and hepatic tryptophan dioxygenase activity by high liquid chromatography. Anal. Biochem. 172, 518–525.
Jafari, R., Almqvist, H., Axelsson, H., Ignatushchenko, M., Lundbäck, T., Nordlund, P., Daniel Martinez Molina, D., 2014. The cellular thermal shift assay for evaluating drug target interactions in cells. Nat. Protoc. 9, 2100–2122.
Johnson, T.S., Munn, D.H., 2012. Host indoleamine 2, 3-dioxygenase: contribution to systemic acquired tumor tolerance. Immunol. Investig. 41, 765–797.
Ketola, K., Hilvo, M., Hyötyläinen, T., Vuoristo, A., Ruskeepää, A.L., Orešič, M., Kallioniemi, O., Iljin, K., 2012. Salinomycin inhibits prostate cancer growth and migration via induction of oxidative stress. Br. J. Cancer 106, 99–106.
Kim, B., 2017. Western blot techniques. Methods Mol. Biol. 1606, 133–139.
Kim, J.H., Chae, M., Kim, W.K., Kim, Y.J., Kang, H.S., Kim, H.S., Yoon, S., 2011a. Salinomycin sensitizes cancer cells to the effects of doxorubicin and etoposide treatment by increasing DNA damage and reducing p21 protein. Br. J. Pharmacol. 162, 773–784.
Kim, K.Y., Yu, S.N., Lee, S.Y., Chun, S.S., Choi, Y.L., Park, Y.M., Song, C.S., Chatterjee, B., Ahn, S.C., 2011b. Salinomycin-induced apoptosis of human prostate cancer cells due to accumulated reactive oxygen species and mitochondrial membrane depolarization. Biochem. Biophys. Res. Commun. 413, 80–86.
Klose, J., Trefz, S., Wagner, T., Steffen, L., Charrier, A.P., Radhakrishnan, P., Volz, C., Schmidt, T., Ulrich, A., Dieter, S.M., Ball, C., Glimm, H., Schneider, M., 2019. Salinomycin: anti-tumor activity in a pre-clinical colorectal cancer model. PLoS One 14, e0211916.
Komiya, T., Huang, C.H., 2018. Updates in the clinical development of epacadostat and other indoleamine 2,3-dioxygenase 1 inhibitors (IDO1) for human cancers. Front. Oncol. 8, 423.
Koo, K.H., Kim, H., Bae, Y.K., Kim, K., Park, B.K., Lee, C.H., Kim, Y.N., 2013. Salinomycin induces cell death via inactivation of Stat3 and downregulation of Skp2. Cell Death Dis. 4, e693.
Koyanagi, M., Kawakabe, S., Arimura, Y., 2016. A comparative study of colorimetric cell proliferation assays in immune cells. Cytotechnology 68, 1489–1498.
Li, J., Xu, W., Yuan, X., Chen, H., Song, H., Wang, B., Han, J., 2017. Polymer-lipid hybrid anti-HER2 nanoparticles for targeted salinomycin delivery to HER2-positive breast cancer stem cells and cancer cells. Int. J. Nanomedicine 12, 6909–6921.
Lin, S.Y., Yeh, T.K., Kuo, C.C., Song, J.S., Cheng, M.F., Liao, F.Y., Chao, M.W., Huang, H.L., Chen, Y.L., Yang, C.Y., Wu, M.H., Hsieh, C.L., Hsiao, W., Peng, Y.H., Wu, J.S., Lin, L.M., Sun, M., Chao, Y.S., Shih, C., Wu, S.Y., Pan, S.L., Hung, M.S., Ueng, S.H., 2016. Phenyl benzenesulfonylhydrazides exhibit selective indoleamine 2,3-dioxygenase inhibition with potent in vivo pharmacodynamic activity and antitumor efficacy. J. Med. Chem. 59, 419–430.
Lu, D., Choi, M.Y., Yu, J., Castro, J.E., Kipps, T.J., Carson, D., 2011. Salinomycin inhibits Wnt signaling and selectively induces apoptosis in chronic lymphocytic leukemia cells. Proc. Natl. Acad. Sci. U. S. A. 108, 13253–13257.
Luo, Q., Yan, L., Xu, P., Xiong, C., Yang, Z., Hu, P., Hu, H., Hong, R., 2018. Discovery of a polysaccharide from the fruiting bodies of Lepista sordida as potent inhibitors of indoleamine 2, 3-dioxygenase (IDO) in HepG2 cells via blocking of STAT1-mediated JAK-PKC-δ signaling pathways. Carbohydr. Polym. 197, 540–547.
Ma, S., Chen, X., Tan, Q., Dai, S., Li, D., Wu, S., Yu, Y., Zang, G., Tang, Z., 2018. An engineered DC-targeting lentivector induces robust T cell responses and inhibits HBV replication in HBV transgenic mice via upregulating T cell autophagy. Cell. Physiol. Biochem. 48, 1041–1059.
Mai, T.T., Hamai, A., Hienzsch, A., Caneque, T., Muller, S., Wicinski, J., Cabaud, O., Leroy, C., David, A., Acevedo, V., 2017. Salinomycin kills cancer stem cells by sequestering iron in lysosomes. Nat. Chem. 9, 1025–1033.
Mao, J., Fan, S., Ma, W., Fan, P., Wang, B., Zhang, J., Wang, H., Tang, B., Zhang, Q., Yu, X., Wang, L., Song, B., Li, L., 2014. Roles of Wnt/β-catenin signaling in the gastric cancer stem cells proliferation and salinomycin treatment. Cell Death Dis. 5, e1039.
Moyer, B.J., Rojas, I.Y., Murray, I.A., Lee, S., Hazlett, H.F., Perdew, G.H., Tomlinson, C.R., 2017. Indoleamine 2,3-dioxygenase 1 (IDO1) inhibitors activate the aryl hydrocarbon receptor. Toxicol. Appl. Pharmacol. 323, 74–80.
Muller, A.J., Prendergast, G.C., 2005. Marrying immunotherapy with chemotherapy: why say IDO? Cancer Res. 65, 8065–8068.
Muller, A.J., DuHadaway, J.B., Donover, P.S., Sutano-Ward, E., Prendergast, G.C., 2005. Inhibition of indoleamine 2,3-dioxygenase, an immunoregulatory target of the cancer suppression gene Bin1, potentiates cancer chemotherapy. Nat. Med. 11, 312–319.
Munn, D.H., Mellor, A.L., 2007. Indoleamine 2, 3-dioxygenase and tumor-induced tolerance. J. Clin. Invest. 117, 1147–1154.
Naujokat, C., Steinhart, R., 2012. Salinomycin as a drug for targeting human cancer stem cells. J. Biomed. Biotechnol. 2012, 950658.
Orabona, C., Pallotta, M.T., Volpi, C., Fallarino, F., Vacca, C., Bianchi, R., Belladonna, M.L., Fioretti, M.C., Grohmann, U., Puccetti, P., 2008. SOCS3 drives proteasomal degradation of indoleamine 2,3-dioxygenase (IDO) and antagonizes IDO-dependent tolerogenesis. Proc. Natl. Acad. Sci. U. S. A. 105, 20828–20833.
Ozaki, Y., Edelstein, M.P., Duch, D.S., 1988. Induction of indoleamine 2,3-dioxygenase: a

mechanism of the antitumor activity of interferon γ. Proc. Natl. Acad. Sci. U. S. A. 85, 1242–1246.
Parajuli, B., Lee, H.G., Kwon, S.H., Cha, S.D., Shin, S.J., Lee, G.H., Bae, I., Cho, C.H., 2013. Salinomycin inhibits Akt/NF-κB and induces apoptosis in cisplatin resistant ovarian cancer cells. Cancer Epidemiol. 37, 512–517.
Perez, R.P., Riese, M.J., Lewis, K.D., Saleh, M.N., Daud, A., Berlin, J., 2017. Epacadostat plus nivolumab in patients with advanced solid tumors: preliminary phase I/II results of ECHO-204. J. Clin. Oncol. 35, 3003 Suppl.
Pilotte, L., Larrieu, P., Stroobant, V., Colau, D., Dolusic, E., Frederick, R., De Plaen, E., Uyttenhove, C., Wouters, J., Masereel, B., 2012. Reversal of tumoral immune resistance by inhibition of tryptophan 2,3-dioxygenase. Proc. Natl. Acad. Sci. U. S. A. 109, 2497–2502.
Platten, M., von Knebel Doeberitz, N., Oezen, I., Wick, W., Ochs, K., 2015. Cancer immunotherapy by targeting IDO1/TDO and their downstream effectors. Front. Immunol. 5, 673.
Qian, S., Zhang, M., Chen, Q.L., He, Y.Y., Wang, W., Wang, Z.Y., 2016. IDO as a drug target for cancer immunotherapy: recent developments in IDO inhbitors discovery. RSC Adv. 6, 7575.
Qiao, H., Chen, X., Chen, E., Zhang, J., Huang, D., Yang, D., Ding, Y., Qian, H., Feijen, J., Chen, E., 2019. Folated pH-degradable nanogels for simultaneous delivery of docetaxel and IDO1-inhibitor in enhancing cancer chemoimmunotherapy. Biomater Sci. 7, 2749–2758.
Rocha, A.J., Miranda, R.S., Sousa, A.J.S., da Silva, A.L.C., 2016. Guidelines for successful quantitative gene expression in real- time qPCR assays. In: Samadikuchaksaraei, Ali (Ed.), Polymerase Chain Reaction for Biomedical Applications. Intech Open, pp. 65850.
Soliman, H., Rawal, B., Fulp, J., Lee, J.H., Lopez, A., Bui, M.M., Khalil, F., Antonia, S., Yfantis, H.G., Lee, D.H., 2013. Analysis of indoleamine 2-3 dioxygenase (IDO1) expression in breast cancer tissue by immunohistochemistry. Cancer Immunol. Immunother. 62, 829–837.
Sotero-Esteva, W.D., Wolfe, D., Ferris, M., Taylor, M.W., 2000. An indoleamine 2,3-dioxygenase-negative mutant is defective in stat1 DNA binding: differential response to IFN-γ and IFN-α. J. Interf. Cytokine Res. 20, 623–632.
Tai, Z.F., Zhang, G.L., Wang, F., 2012. Identification of small molecule activators of the Janus kinase/signal transducer and activator of transcription pathway using a cell-based screen. Biol. Pharm. Bull. 35, 65–71.
Tominaga, H., Ishiyama, M., Ohseto, F., Sasamoto, K., Hamamoto, T., Suzuki, K., Watanabe, M., 1999. A water-soluble tetrazolium salt useful for colorimetric cell viability assay. Anal. Commun. 36, 47.
Torre, L.A., Islami, F., Siegel, R.L., Ward, E.M., Jemal, A., 2017. Global cancer in women: burden and trends. Cancer Epidemiol. Biomark. Prev. 26, 444–457.
Tyagia, M.B., Patro, S., 2019. Salinomycin reduces growth, proliferation and metastasis of cisplatin resistant breast cancer cells via NF-κB deregulation. Toxicol. in Vitro 60, 125–133.
Vogel, C.F.A., Goth, S.R., Dong, B., Pessah, I.N., Matsumura, F., 2008. Aryl hydrocarbon receptor signaling mediates expression of indoleamine 2,3-dioxygenase. Biochem. Biophys. Res. Commun. 375, 331–335.
Wright, E.J., De Castro, K.P., Joshi, A.D., Elferink, C.J., 2017. Canonical and non-canonical aryl hydrocarbon receptor signaling pathways. Curr Opin Toxicol. 2, 87–92.
Xue, P., Fu, J., Zhou, Y., 2018. The aryl hydrocarbon receptor and tumor immunity. Front. Immunol. 9, 286.
Yang, H., Pawitan, Y., He, W., Eriksson, L., Holowko, N., Hall, P., Czene, K., 2019a. Disease trajectories and mortality among women diagnosed with breast cancer. Breast Cancer Res. 21, 95.
Yang, L., Chen, Y., He, J., Njoya, E.M., Chen, J., Liu, S., Xie, C., Huang, W., Wang, F., Wang, Z., Li, Y., Qian, S., 2019b. 4,6-substituted-1H-Indazoles as potent IDO1/TDO dual inhibitors. Bioorg. Med. Chem. 27, 1087–1098.
Ye, Z., Yue, L., Shi, J., Shao, M., Wu, T., 2019. Role of IDO and TDO in cancers and related diseases and the therapeutic implications. J. Cancer 10, 2771–2781.
Yu, J., Wang, Y., Yan, F., Zhang, P., Li, H., Zhao, H., Yan, C., Yan, F., Ren, X., 2014. Noncanonical NF-κB activation mediates STAT3-stimulated IDO upregulation in myeloid-derived suppressor cells in breast cancer. J. Immunol. 193, 2574–2586.
Yue, E.W., Sparks, R., Polam, P., Modi, D., Douty, B., Wayland, B., Glass, B., Amy, T., Glenn, J., Zhu, W., Bower, M., Liu, X., Leffet, L., Wang, Q., Bowman, K.J., Hansbury, M.J., Wei, M., Li, Y., Wynn, R., Burn, T.C., Koblish, H.K., Fridman, J.S., Emm, Tom, Scherle, P.A., Metcalf, B., Combs, A.P., 2017. INCB24360 (Epacadostat), a highly potent and selective indoleamine-2,3-dioxygenase 1 (IDO1) inhibitor for immune-oncology. ACS Med. Chem. Lett. 85486–85491.
Zhai, L., Spranger, S., Binder, D.C., Gritsina, G., Lauing, K.L., Giles, F.J., Wainwright, D.A., 2015. Molecular pathways: targeting IDO1 and other tryptophan dioxygenases for cancer immunotherapy. Clin. Cancer Res. 21, 5427–5433.
Zhang, P., Jiang, G., Gao, J., Li, L., Du, J., Jiao, X., 2013. SAHA down-regulates the expression of indoleamine 2,3-dioxygenase via inhibition of the JAK/STAT1 signaling pathway in gallbladder carcinoma cells. Oncol. Rep. 29, 269–275.
Zhao, Y., Zhao, W., Lim, Y.C., Liu, T., 2019. Salinomycin-loaded gold nanoparticles for treating cancer stem cells by ferroptosis-induced cell death. Mol. Pharm. 16, 2532–2539.
Zhou, S., Wang, F., Wong, E.T., Fonkem, E., Hsieh, T., Wu, J.M., Wu, E., 2013. Salinomycin: a novel anti-cancer agent with known anti-coccidial activities. Curr. Med. Chem. 20, 4095–4101.